Experimental Study of the Viscous Sublayer in Turbulent Pipe Flow

A. T. POPOVICH and R. L. HUMMEL

University of Toronto, Toronto, Ontario, Canada

A flash photolysis method for nondisturbing turbulent flow measurements has been applied to study conditions in the viscous sublayer in a square smooth pipe. Experimental results are obtained that are extremely difficult to obtain by any other known technique.

The results show that, adjacent to the wall, there is a layer of very small thickness $y^+ = 1.6 \pm 0.4$ in which a linear velocity gradient occurs virtually at all times, but the slope of the gradient changes with time. Beyond $y^+ = 34.6$ essentially turbulent flow exists. In the transition region in between, very disturbed flow conditions prevail. However, the technique used clearly indicates the instantaneous velocity distribution in the flow field bewteen the wall and the fully turbulent region.

Statistical distributions of the instantaneous wall shear stress (evaluated from the slope of the velocity gradient), the laminar sublayer thickness, and the velocity at the edge of the laminar sublayer are obtained. It follows that the partial turbulence mechanism whereby the flow at a point is turbulent only a fraction of the time is, at least to an extent, responsible for the reduction of eddy diffusivity by kinematic viscosity close to the wall.

Experimental velocity profile obtained in the present investigation is compared with the proposed and experimental velocity profiles of other authors.

It has long been recognized that the velocity in a moving fluid in contact with a solid body changes continuously from a small value near the wall to a maximum away from the wall. As early as 1738 (*1*) Daniel Bernoulli had expressed the view that a real fluid could not slip freely over the surface of a solid body. Speculations about the real nature of the flow in the thin layer adjacent to the body, however, have been going on ever since. More than one hundred and fifty years after Bernoulli, Prandtl developed a theory of wall turbulence, where the existence of a laminar sublayer was the requirement for evaluating an integration constant in the equation of velocity distribution.

Fage and Townend (*2*) and Fage (*3*) seem to have been the first to examine experimentally flow conditions in the viscous sublayer. They observed the motion of extremely small dust particles in water under the ultramicroscope and found no evidence of the existence of a region possessing rectilinear motion.

Gas flow measurements in the viscous sublayer by the Pitot tube and hot-wire methods were published by Reichardt (*4*) in 1940, By Deissler (*5, 6*) in 1950, and by Laufer (*7*) in 1953. The data for the mean velocity distribution show some scatter. The hot-wire method is not a direct method for velocity measurements. Some disturbances in the flow are produced especially when the hot wire is used for measurements near the wall where corrections of the results are necessary. Thus, it is not certain that the results are quite accurate.

Most recently (*8*) velocity measurements in turbulent pipe flow have been made by the particle method. Both the instantaneous and average velocities were obtained, but for distances from the wall corresponding to those beyond the commonly defined sublayer. The average velocity profile in the region between $y^+ = 18$ and $y^+ = 57$ lies markedly below the profiles obtained by both the Pitot tube and the hot-wire method.

An interesting but, unfortunately, only qualitative experiment has been performed independently by Einstein and Li (*9*) and by Sackmann and Hettler (*10*). A dye is injected into the viscous sublayer through a small hole drilled into the bottom wall of a pipe. It is observed that the dye is either mixed with the turbulent flow almost instantly or it is carried downstream for some time before mixing occurs. It is most interesting that the given explanations for these observations differ. Einstein and Li express the view that the dye will either mix with the turbulent flow or not, depending on whether at that point the laminar sublayer decays or is in the period of growth. On the other hand, Sackmann and Hettler state that the dye injected into the laminar sublayer will not mix with the turbulent flow if the injection pressure matches correctly the pressure in the flowing fluid, that is, if the laminar sublayer is not disturbed.

Whereas the available experimental velocity profiles are not accurate enough very near the wall to make possible a reliable determination of the thickness of the laminar sublayer, Lin et al. (*11*) have made use of the concentration profiles at high Schmidt numbers to conclude that there is no "definite laminar film" through which a pure molecular diffusion would take place near the wall.

In spite of all the work done so far, our knowledge about the flow conditions in the viscous sublayer is still incomplete. It is expressed by Kay (*12*) as follows: "Doubts have been expressed regarding the validity of the original experimental observations which gave the figure of $y^+ = 5$ for the thickness of the true laminar sublayer. Other indirect measurements, however, have tended to support this figure. It has also been suggested that the laminar sublayer is not in fact of constant thickness but that it oscillates in an irregular manner."

The main reason for the existing inadequate knowledge of the viscous sublayer is, of course, the lack of a suitable experimental technique. However, a new method for observing the flow conditions in the viscous sublayer has been developed (*13*) which has the potentiality of providing a better understanding of the sublayer. Some of the results obtained by the method are presented here.

A. T. Popovich is at Laval University, Quebec, Canada.

EXPERIMENTAL APPARATUS

The details about the flash photolysis technique used for observing the flow conditions in the viscous sublayer have been given elsewhere (*14*). A colored tracer in the form of a parallelepiped, approximately 5 mm. long, 0.1 mm. wide, and 0.5 mm. deep, beginning at the wall was introduced into the photosensitive fluid by focusing the light from a Xenon flash tube, onto the test section of a pipe. The experiments were made on flow of 95% ethanol, containing 0.1% by weight of 2-(2,4-dinitro-benzyl)-pyridine, in a square aluminum alloy smooth pipe with a side of dimension 2.06 and 160.5 cm. long. The fluid was flowing between two constant head reservoirs with a 90-deg. elbow mounted at the entrance of the pipe. The test section was located 116 cm. downstream from the entrance of the pipe. It consisted of three 1/16-in. thick quartz plates inserted in, and replacing, three adjacent sides of the channel to allow the introduction, illumination, and observation of the tracers. The plates were connected to the pipe by Shell Epon Resin 828, with its inner surfaces flush with those of the channel. The tracer was introduced in the middle of the vertical side of the channel 10.7 cm. from the upstream end of the quartz window and was filmed on a Kodak High Contrast Copy film with a Nikon F, 55 mm. camera provided with a Nikon Bellows Focusing attachment which gave 1.93X magnification.

RESULTS AND DISCUSSION

The tracer was observed in two dimensions. When filmed at the instant of formation it appeared as a straight line approximately 1 mm. long and 0.1 mm. wide beginning at, and perpendicular to, the wall. One hundred and forty-seven photographs of the tracer were taken under the same conditions (U_{av} = 102.5 cm./sec., $N_{Re} = U_{av}\,2S/\nu$ = 13,100 at 24°C.), 1.4 msec. after the formation. The time interval between the successive shots was 1.5 min.

It is concluded that almost all traces have been truncated at the farthest end from the wall by a violent turbulent motion. The remaining portion, however, could be clearly followed. Far from appearing the same in all photographs, the shape and form of the trace differed. It was possible to classify them into several groups as shown in Table 1. All the flow patterns found in the viscous sublayer are well represented by the shown traces, with only one additional observation that the angle between the trace and the wall varies incessantly with time. It is seen that the usually pictured (number I*a* in Table 1) velocity profile in the laminar sublayer is found in only 38.1% of measurements. An additional 7.5% of the photographs show pure shear in the region but with continuously changing velocity gradient (number II*a*), and the remaining 54.4% indicate the presence of some turbulent motion or three-dimensional distortion. Only flow pattern III reveals that for a fraction of the time strong eddies are also present near the wall. It is obviously important to know how close the strong eddies come to the wall, since the rates of mass and heat transfer from the wall are very much influenced by them. Flow pattern III is, therefore, analyzed separately and the results are presented in Table 2, with the mean value $y^+ = 5.05$.

In the present work it has not even once been observed that the strong eddies would reach the wall itself. The closest distance to the wall reached by the eddies has been $y^+ = 2.09$ with an accuracy of reading the distances on pictures of ± 0.2.

TABLE 1. CLASSIFICATION OF FLOW PATTERNS IN VISCOUS SUBLAYER

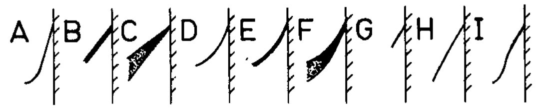

	TYPE DESIGNATION	FORM OF TRACE	NUMBER OF PHOTOGRAPHS SHOWING A PARTICULAR TRACE FORM, TOTAL N° N=147
A	Ia	NORMAL PURE SHEAR	56
B	Ib	NORMAL SLIGHTLY BROADENED	10
C	Ic	NORMAL BROADENED	13
D	IIa	PARABOLIC PURE SHEAR	11
E	IIb	PARABOLIC SLIGHTLY BROADENED	10
F	IIc	PARABOLIC BROADENED	27
G	III	SWEPT AWAY BY STRONG EDDIES	15
H	IV	INVERSE PARABOLIC	2
I	V	POSSESSING A KINK	3

TABLE 2. OBSERVED INSTANTANEOUS DISTANCES FROM STRONG EDDIES TO WALL

δ_L μ	$\frac{x_2}{S}$	y^+
156	0.015	6.29
132	0.013	5.32
91	0.009	3.67
185	0.018	7.46
132	0.013	5.32
237	0.023	9.56
131	0.013	5.28
146	0.014	5.89
87	0.008	3.50
137	0.013	5.53
52	0.005	2.09
128	0.012	5.16
116	0.011	4.68
64	0.006	2.58
87	0.008	3.50

THE THICKNESS OF THE LAMINAR SUBLAYER

We shall define in this work the instantaneous thickness of the laminar sublayer as that portion of the velocity profile on each photograph that can be approximated by a straight line starting from the wall.

It is, then, clearly seen from the photographs obtained with the present technique that both the velocity and the thickness of the laminar sublayer vary with time. The results are presented in Figures 1 and 4. The statistical distribution curve of the thickness of the laminar sublayer, in Figure 1, is skewed with very large values of δ_L occurring occasionally. The average thickness of the laminar sublayer is $\overline{\delta_L} = 153\mu$ corresponding to $y^+ = 6.17$, but

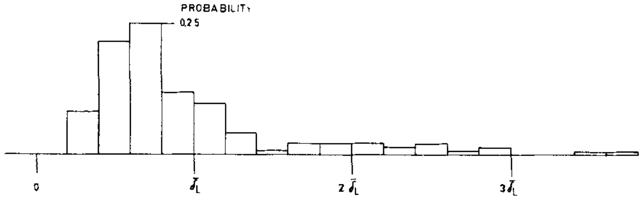

Fig. 1. Statistical distribution of the thickness of laminar sublayer ($N = 147$).

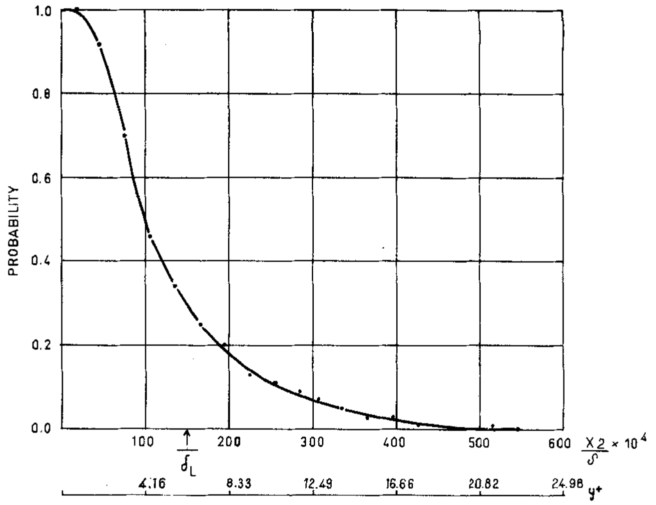

Fig. 2. Probability of occurrence of laminar flow at a distance x_2/S.

the most probable thickness is considerably smaller, namely, $0.7\ \overline{\delta}_L = 107\mu$, $y^+ = 4.3$.

It follows that the flow at a point is turbulent only a fraction of the time. The probability of occurrence of laminar flow in the region between the wall and a distance x_2/S is presented in Figure 2. Adjacent to the wall there is a very thin layer of thickness $y^+ = 1.6 \pm 0.4$ in which the velocity gradient on all one hundred and forty-seven photographs is essentially linear, but the slope of the gradient changes with time.

THE REGIONS OF THE VISCOUS SUBLAYER

Although the division of the viscous sublayer into regions does not contribute to the understanding of the mechanism of momentum exchange between the wall and the turbulent core, it has proved useful for the evaluation of heat and mass transfer in turbulent flow. It should be, therefore, of some interest to report the magnitudes of the distances between the wall and some characteristic points on the instantaneous velocity distribution curves in the viscous sublayer, inasmuch as the technique used is a direct, nondisturbing method for flow measurements.

As mentioned in the preceding section, the distance $y^+ = 1.6 \pm 0.4$ from the wall includes the region of essentially linear velocity gradient with the slope of the gradient changing with time.

The maximum distance from the wall at which the trace could still be observed was found to be $x_2 = 860\mu$ or $y^+ = 34.6$. It is concluded that beyond this point the flow is practically turbulent at all times.

On all one hundred and forty-seven photographs there was a point at which either the velocity gradient changed its value sharply or the trace disappeared. The average value of these distances was $x_2 = 300\mu$ corresponding to $y^+ = 12.1$. The described regions are summarized in Table 3. In the same table, the percent of the total number of photographs is given, which pictures, in turn, linear velocity gradient, curved velocity gradient, and turbulent flow in each region. The distance $y^+ = 12.1$ divides the flow field into the first and second transition region. In the first transition region the flow is only occasionally turbulent, and in the second transition region the flow is predominantly turbulent.

THE WALL SHEAR STRESS

Stanton (*15*) and Fage (*16*) have measured the mean velocity in a turbulent pipe flow very close to the wall employing specially designed surface tubes. They have reported that with this measurement used the wall shear stress can be determined from the relation $\tau_o = \mu\left(\frac{\partial \overline{U}_1}{\partial x_2}\right)_{x_2=0}$, although the flow had been found not to be regular near the wall. Elaborate corrections and calibrations were necessary to obtain the proper result.

Quite recently Tu and Willmarth (*17*) have calculated the mean wall shear stress using the same relation as Stanton, but the velocity was measured with the hot wire rather than with the surface tube. Again, corrections were required to get accurate results.

The technique used in this work is unique in that it makes possible the evaluation of the instantaneous value of the wall shear stress from the experimentally determined slope of the velocity gradient in the laminar sublayer. The instantaneous wall shear stresses have been evaluated on all one hundred and forty-seven photographs and the results are presented in Figure 3. The average $\overline{\tau}_o$

TABLE 3. FLOW CONDITIONS IN REGIONS OF VISCOUS SUBLAYER

		Region				
		1 Laminar sublayer	11 Transition	111 Turbulent	11*a* First transition	11*b* Second transition
		$y^+ = 0 - (1.6 \pm 0.4)$	$y^+ = (1.6 \pm 0.4) - 34.6$	$y^+ \geqq 34.6$	$y^+ = (1.6 \pm 0.4) - 12.1$	$y^+ = 12.1\text{-}34.6$
No. of pictures showing a particular flow condition in percent of total number, $N = 147$	Linear velocity gradient	100.0	20.5	0	46.9	4.8
	Curved velocity gradient	0	62.7	0	46.7	59.5
	Turbulent flow	0	16.7	100	6.4	35.7

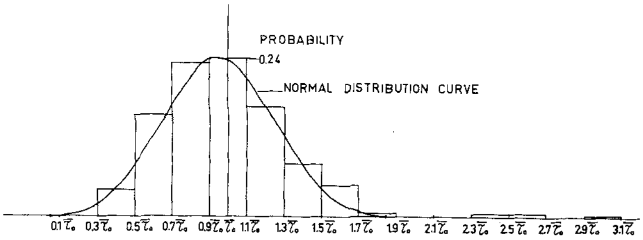

Fig. 3. Statistical distribution of the wall shear stress (N = 147).

$= 33.9$ (g.)(cm.)/(sec.^{2})(sq.cm.) and the statistical distribution of τ_o, unlike that for the laminar sublayer, follows the normal distribution curve with the most probable $\tau_o = 0.95\bar{\tau}_o = 32.2$ (g.)(cm.)/(sec.^{2})(sq.cm.). When one uses the empirical equation $\bar{\tau}_o = f\dfrac{\rho\, U^2_{av}}{8}$, the wall shear stress can be calculated, giving $\bar{\tau}_o = 0.029\dfrac{0.800(102.5)^2}{8}$ $= 30.5$ (g.)(cm.)/(sec.^{2})(sq.cm.), which, in accordance with the experimental results on Figure 3, still belongs to the most frequently occurring values. In all the calculations done in this work, the value $\bar{\tau}_o = 33.9$ is used (*13*).

THE INSTANTANEOUS VELOCITY PROFILE

The flash photolysis method employed in the present work provides a means of direct determination of the instantaneous velocity profile in the whole region of the viscous sublayer without the slightest disturbance of the flow. The mean values at any desired distance from the wall can then be determined by averaging all the instantaneous readings at that point. These are obtained by dividing the traveled distance by the elapsed time. The distance could be read from photographs with a precision of $\pm$ 5μ, and the time interval was predetermined by a time-delay electronic circuit calibrated with an oscilloscope precisely to about 1%.

The instantaneous velocities at the edge of the laminar sublayer $U_{1,\max}$, are plotted against the sublayer thickness in Figure 4. A straight line connecting the origin with any of these points makes it possible to read an instantaneous velocity at any distance between the wall and that point. The average value of all $U_{1,\max}$ is found to be, in these experiments, $\bar{U}_{1,\max} = 37.4$ cm./sec. For comparison, the same quantity obtained in this work from the average slope of the velocity gradient at the wall and the average sublayer thickness is 40.2 cm./sec.

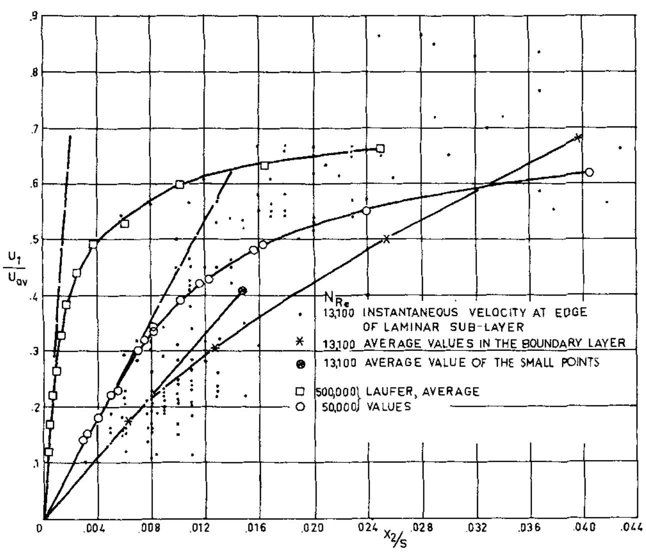

Fig. 4. Velocity distribution near wall.

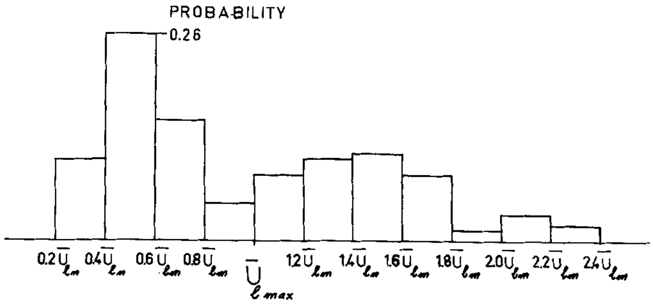

Fig. 5. Statistical distribution of instantaneous velocity at edge of laminar sublayer (N = 147).

The statistical distribution of $U_{1,\max}$ is shown in Figure 5. It is similar to that for δ_L but shows two maxima: one at $0.5\bar{U}_{1,\max}$ and the other at about 1.4 $\bar{U}_{1,\max}$.

THE MEAN VELOCITY DISTRIBUTION

Measurements of the mean velocity distribution in the viscous sublayer have been made by several authors, using the hot-wire method and to some extent the Pitot tube and particle methods. It appears, however, that for the first time in this work the velocity distribution very close to the wall has been obtained by a method which does not require any correction for interference with the flow: It should be useful, therefore, to compare these measurements with the results of other authors, as well as with the proposed curves for the velocity distribution.

A fairly complete summary of the expressions for eddy viscosity, which form the basis for the derivation of the velocity distribution functions, is given by Rotta (*18*) and will not be repeated here. We shall only mention three additional publications as follows.

Rannie (*19*) has attempted to find a relation for eddy viscosity that would lead to the same variation of heat transfer with Prandtl number as that obtained by experiment. The proposed relation is

$$\frac{\epsilon}{\nu} = \sinh^2 (\sqrt{K_1}\; y^+)$$

where K_1 is a constant.

Hanratty's (*20*) equation for velocity distribution

$$u^+ = 13.5 \int_0^1 \operatorname{erf} \frac{y^+ \sqrt{\pi}}{13.5 \times 4 \times (\theta/\theta_c)^{1/2}}\, d(\theta/\theta_c)$$

was obtained on the main assumption that a continuous laminar sublayer did not exist in turbulent flow. The model, proposed earlier by Dankwerts, pictured a continual change of the fluid in contact with the wall. The

TABLE 4. AVERAGE QUANTITIES OBTAINED BY FLASH PHOTOLYSIS METHOD (Present Investigation)

x_2 (μ)	$\dfrac{x_2}{S}$	$\dfrac{x_2 u^*}{\nu}$	$\log\dfrac{x_2 u^*}{\nu}$	$\bar{U}_1$ cm./sec.	$\dfrac{\bar{U}_1}{u^*}$	$\dfrac{\bar{U}_1}{U_{av}}$
64.3	0.0062	2.6	0.415	18.7	2.87	0.182
130.3	0.0126	5.3	0.722	31.0	4.76	0.300
260.0	0.0252	10.5	1.022	50.9	7.82	0.500
407.7	0.0396	16.5	1.217	69.8	10.73	0.681

TABLE 5. AVERAGE QUANTITIES OBTAINED BY PARTICLE METHOD (8)
(THE VALUES ARE OBTAINED FROM FIGURE 12)

$\frac{x_2 u^*}{\nu}$	$\log \frac{x_2 u^*}{\nu}$	$\overline{U}_1/u^*$
5.8	0.76	5.0
9.3	0.97	7.0
16.3	1.21	10.5
23.5	1.37	11.5
30.0	1.48	12.7
37.5	1.57	13.25
44.0	1.64	13.9
53.0	1.72	14.7
69.0	1.84	15.6

mean velocity values, at any point, were very much dependent on the ratio of the velocity, at a characteristic point near the wall, to the friction velocity. Because of the lack of knowledge regarding the true flow conditions in the viscous sublayer, the ratio was chosen more or less arbitrarily. It should be noted that, as Hanratty pointed out, his expression is expected to hold only for values of y^+ much less than 30, owing to the boundary conditions selected.

The fact that a simple, easily evaluated, single formula for the law of the wall has not been proposed has prompted Spalding (21) to look for a relation giving y^+ explicitly in terms of u^+ instead of vice versa as is usually done. He has proposed three equations, the simplest of which is

$$y^+ = u^+ + 0.1108\,(e^{0.4u^+} - 1 - 0.4u^+)$$

It contains both the universal velocity distribution law and the law for purely laminar friction, plus two completely empirical terms. We shall refer to it as Spalding's equation (5) as marked in his publication. The other two equations contain additional terms, introduced in order to fit the available experimental data.

To compare the proposed curves for velocity distribution with the results of the present experimental investigation, the average velocities at four selected distances from the wall have been determined in this work as shown in Table 4. The results obtained by the particle method (8) are presented in Table 5.

The curve in Figure 6 is given by Reichardt (4). Plotted on the figure are the data of Nikuradse, obtained by Pitot tube, of Reichardt, obtained by Pitot tube and the hot wire, of Hettler obtained by the particle method, and of the present investigation where the flash photolysis method has been applied. Although the hot-wire and Pitot tube measurements show some scatter, it is seen that the data obtained by four different methods agree fairly well with the proposed curve up to a distance of about $y^+ = 17$ from the wall. The agreement between the particle and flash photolysis methods in this region is excellent. Between $y^+ = 17$ and approximately $y^+ = 56$, however, the values obtained by the particle method lie markedly lower than the hot-wire and Pitot tube data. Since the agreement between the particle and the available flash photolysis measurements has been so good, we are tempted to conclude that the present investigation would support the particle method rather than the hot-wire or Pitot tube data. It should be noted, however, that the trace produced in the photosensitive fluid was not observed on all photographs beyond about $y^+ = 17$, and thus the measurements in this region could not be made.

Rotta's (22) equation overestimates the magnitudes of the mean velocities in the transition region as shown in

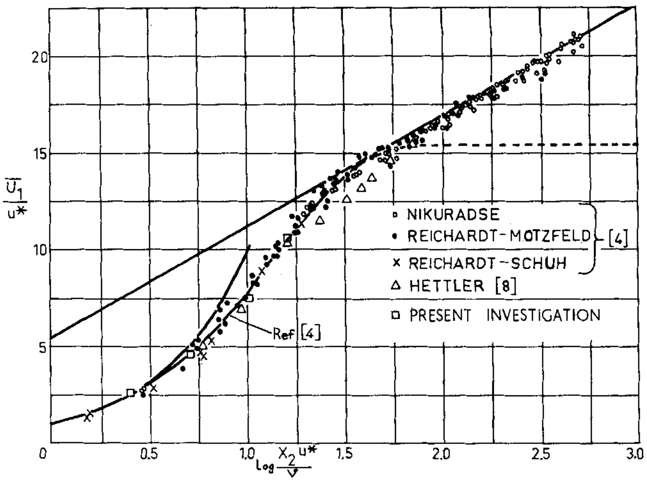

Fig. 6. Comparison of Reichardt's curve with measured velocity profiles.

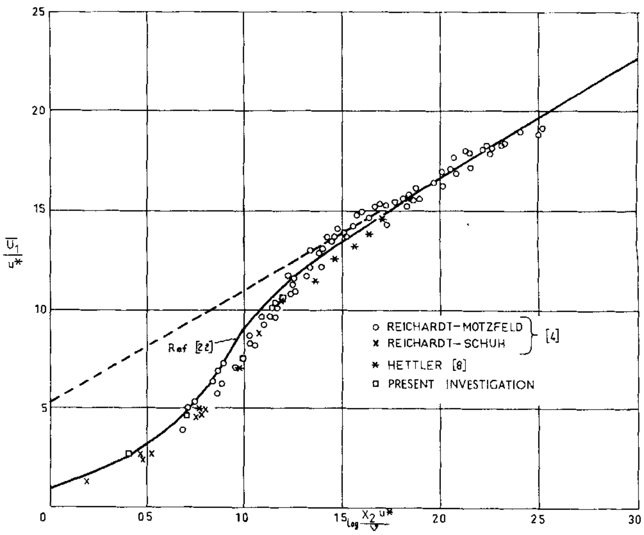

Fig. 7. Comparison of Rotta's curve with measured velocity profiles.

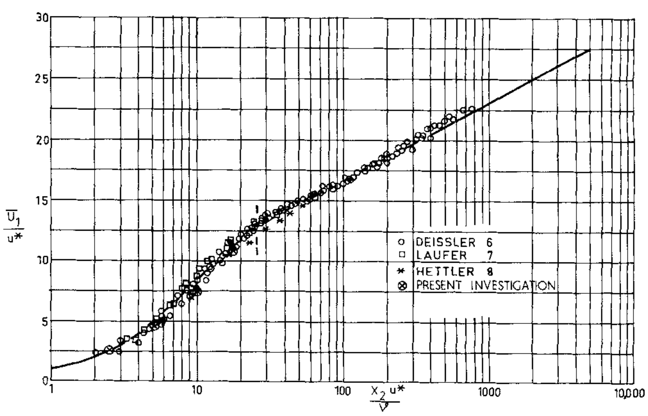

Fig. 8. Comparison of Deissler's curves with measured velocity profiles.

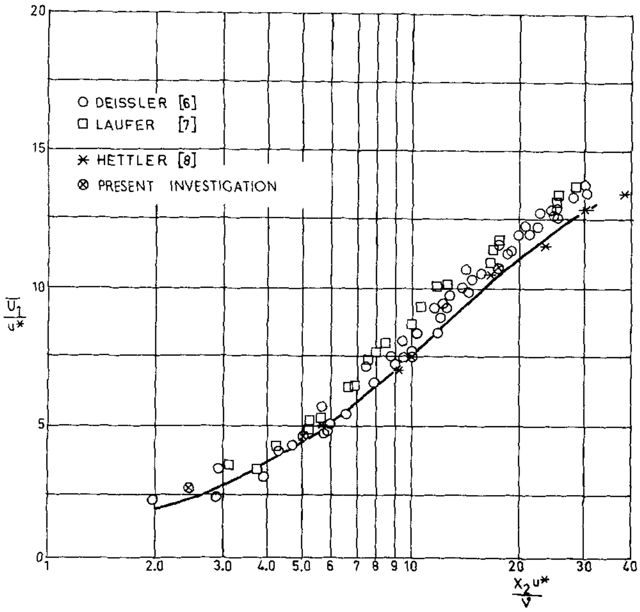

Fig. 9. Comparison of data with Harratty's theory.

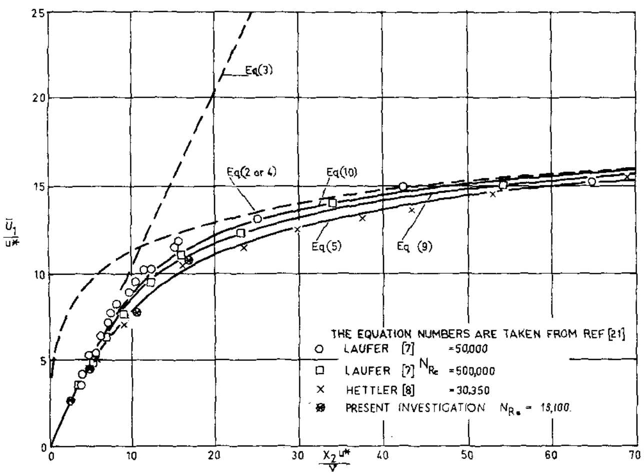

Fig. 10. Average velocity distribution near wall compared with Spalding's equations.

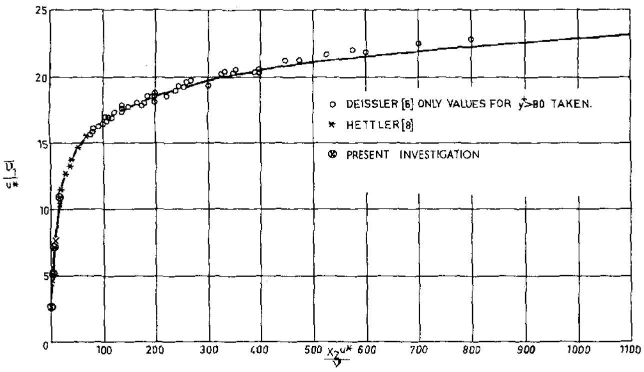

Fig. 11. Comparison of velocity profile in wall turbulence with Spalding's equation (5).

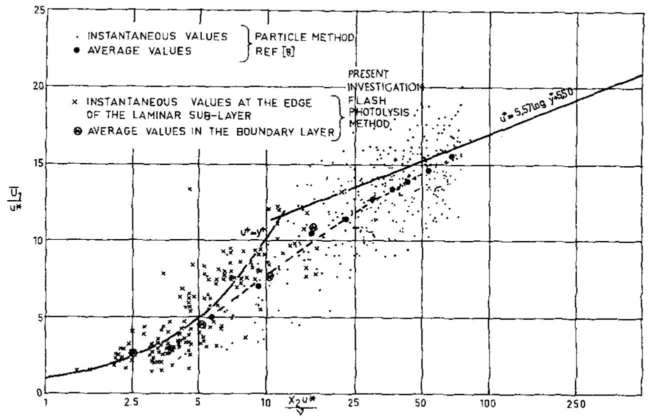

Fig. 12. Comparison of experimental results obtained by particle and flash photolysis methods.

Figure 7 and so does, to a lesser extent, Deissler's (*6*) curve presented in Figure 8.

The experimental results are compared with Hanratty's theory in Figure 9. If one follows Hanratty's criterion for choosing the value of the ratio $u_L/\sqrt{\tau_o/\rho}$ as that at the end of the transition region, practically the same curve is obtained on the basis of the experimental velocity profile found in this work ($u^+ = 13.3$ compared with Hanratty's $u^+ = 13.5$). The equation fits well the measurements obtained by the particle method and the available flash photolysis data, in spite of the inappropriate boundary conditions and uncertain assumptions made in its derivation.

Figure 10 shows the agreement between Spalding's equation and the measurements of Laufer (*7*), Hettler (*8*), and the present investigation. Spalding's equation (*5*) is drawn for a very wide region of wall turbulence in Figure 11, on which the available data obtained by the particle and flash photolysis methods are plotted. Deissler's measurements for the region beyond $y^+ = 80$ are also shown. Hettler's data lie exactly on the curve. Again, flash photolysis measurements seem to support this finding, but the maximum distance from the wall reached is approximately $y^+ = 17$.

Instantaneous values at the edge of the laminar sublayer and the average values of the velocities near the wall obtained by the flash photolysis method are shown with Hettler's results in Figure 12. It is seen that the agreement between the available data is quite satisfactory.

NOTATION

e = base of the natural logarithms
N = total number of photographs
N_{Re} = $U_{av}2s/\nu$, Reynolds number
S = half of the inner side of square pipe, L
U_{av} = mean velocity in the pipe L/T
U_1 = instantaneous velocity at a point in the axial direction of pipe L/T
$\overline{U_1}$ = average value of U_1, L/T
$U_{1,max}$ = instantaneous velocity at the edge of laminar sublayer, L/T
$\overline{U}_{1,max}$ = average value of $U_{1,max}$, L/T
u^* = $(\tau_o/\rho)^{1/2}$, L/T
u^+ = U_1/u^*, dimensionless velocity
u_L = velocity in axial direction of fluid mass before contact with the wall
x_2 = shortest distance from the wall, L
y^+ = x_2u^*/ν, shortest dimensionless distance from wall

Greek Letters

δ_L = thickness of laminar sublayer, L

ϵ = eddy viscosity, L^2/T
μ = viscosity, M/LT or length dimension, micron
ν = μ/ρ, L^2/T
ρ = density M/L^3
$\bar{\tau}_0$ = average wall shear stress, ML/T^2L^2
θ = time, T
θ_c = total time for which a fluid mass had been in contact with the wall, T

LITERATURE CITED

1. Goldstein, S., ed., "Modern Developments in Fluid Mechanics," p. 676, Oxford Univ. Press (1938).
2. Fage, A., and H. C. H. Townend, *Proc. Roy. Soc.* (*London*), **135**, 656 (1932).
3. Fage, A., *Phil. Mag.*, **21**, 80 (1936).
4. Reichardt, H., *Z.A.M.M.*, **20**, 297 (1940).
5. Deissler, R. G., *Natl. Advisory Comm. Aeronaut. Tech. Note 2138* (1950).
6. *Ibid.*, *3145* (1954).
7. Laufer, John, *Natl. Advisory Comm. Aeronaut. Tech. Rept. 1174* (1954).
8. Hettler, J.-P., P. Muntzer, and O. Scrivener, *Compt. Rend.*, **258**, 4201 (1964).
9. Einstein, H. A., and Huon Li, *Proc. Am. Soc. Civ. Engrs.*, Paper 945 (1956).
10. Sackmann, L. A., and J.-P. Hettler, *Compt. Rend.*, **251**, 2874 (1960).
11. Lin, C. S., R. W. Moulton, and G. L. Putnam, *Ind. Eng. Chem.*, **45**, 636 (1953).
12. Kay, J. M., "An Introduction to Fluid Mechanics and Heat Transfer," p. 184, Cambridge Univ. Press (1963).
13. Popovich, A. T., Ph.D. thesis, Univ. Toronto (1966).
14. ———, and R. L. Hummel, *Chem. Eng. Sci.*, **22**, 21 (1967).
15. Stanton, T. E., *Proc. Roy. Soc. (London)*, **A97**, 413 (1920).
16. Fage, A., *J. Aeronaut. Sci.*, **1**, 35 (1934).
17. Bo-Jang, Tu, and W. W. Willmarth, *Tech. Rept.*, Univ. Michigan, Ann Arbor, Appendix III (1966).
18. Rotta, J. C., "Progress in Aeronautical Sciences," p. 79, Pergamon Press, New York (1962).
19. Rannie, W. D., *J. Aeronaut. Sci.*, **23**, 485 (1956).
20. Hanratty, T. J., *AIChE J.*, **2**, 359 (1956).
21. Spalding, D. B., *J. Appl. Mech.*, **28**, 455 (1961).
22. Rotta, J. C., *Ing. Arch.*, **18**, 277 (1950).

Manuscript received April 28, 1966; revision received October 10, 1966; paper accepted October 24, 1966. Paper presented at AIChE Detroit meeting.

Transport of Gases Through Insoluble Monolayers

EIZO SADA and D. M. HIMMELBLAU

University of Texas, Austin, Texas

The reduction in gas desorption through surface active monolayers on a water substrate has been investigated for five compounds (1-hexadecanol, 1-octadecanol, 1-docosanol, 1-eicosanoic acid, and 1-docosanoic acid) and four gases (oxygen, nitrogen, methane and carbon dioxide) at 25°C. Gas transport was retarded significantly at high surface coverage and decreased nonlinearly with change in surface coverage past the point equivalent to zero surface pressure.

Interphase mass transfer coefficients for transport through the films were calculated, but no simple correlation could be discovered which could be used to predict film coefficients or the reduction as a function of surface coverage.

Insoluble monolayers which occur naturally on bodies of water, and which are introduced occasionally by man to retard evaporation, also may suppress the transport of respiratory and toxic gases through gas-liquid interfaces. Diffrences have been noted between the permeability of monolayers to gases such as carbon dioxide, oxygen, and nitrogen, and the permeability to water vapor. LaMer (9) has summarized some of the interesting properties of monolayers in the retardation of evaporation and its importance in water conservation. It has been demonstrated that transport of water through compressed monolayers is not solely a diffusion process but must be treated as a combined process of diffusion and reaction (or adsorption) at the monolayer.

Some of the earliest work in the field dealing with a dissolved substance in water was by Langmuir and Langmuir (*10*), who reported on the evaporation of ethyl ether from water through oleic acid monolayers, but the effect noted was that the ether primarily prevented enhanced transport in the liquid by reducing convection in the liquid. Sebba and Rideal (*14*) studied the effect of monolayers on the evaporation of ethanol and ammonia.

More recently Blank and Roughton (3) reported on the results of their work in the absorption of oxygen and carbon dioxide through monolayers into reacting solutions. Blank (*2*) also has investigated the transfer of oxygen, carbon dioxide, nitrous oxide, and sulfur dioxide with and without monolayers from the gas to the liquid phase as a

E. Sada is at the University of Nagoya, Chikusa, Japan.